MATERIALS ENGINEERING

Crystallization of low silica Na-A and Na-X zeolites from transformation of kaolin and obsidian by alkaline fusion

INGENIERÍA DE MATERIALES

Cristalizacion de zeolitas Na-A y Na-X bajas en sílice a partir de la transformación de caolín y obsidiana por fusión alcalina

Carlos A. Ríos[*], Craig D. Williams[**] and Oscar M. Castellanos[***] §

[*] *Escuela de Geología, Universidad Industrial de Santander, Colombia,*
[**] *School of Applied Sciences, University of Wolverhampton, England,*
[***] *Programa de Geología, Universidad de Pamplona, Colombia*

§ carios@uis.edu.co, c.williams@wlv.ac.uk, oscarmca@yahoo.es

(Recibido: Diciembre 12 de 2011 – Aceptado: Noviembre 01 de 2012)

Abstract

Zeolites Na-A and Na-X were successfully synthesized from kaolin and obsidian, respectively, following the alkaline fusion method. Raw materials were hydrothermally activated with NaOH to synthesize zeolites Na-A and Na-X. The transformation of the starting materials into zeolites has been evaluated by powder X-ray diffraction, scanning electron microscopy and Fourier transformed infrared spectroscopy to elucidate the crystallization process of zeolites. The use of low cost materials in zeolite synthesis become an area of important interest and research, playing an active role in promoting technological advances, research and technology transfer related to the production of zeolytic materials under well-optimized experimental conditions.

Keywords: *Aluminosilicates, Crystallization, Fusion, Hydrothermal, Zeolites*

Resumen

En el presente estudio se llevó a cabo la síntesis de zeolitas Na-A y Na-X a partir de caolín y obsidiana, respectivamente, siguiendo el método de fusión alcalina. Los materiales de partida fueron activados hidrotérmicamente con NaOH para sintetizar productos de alta pureza. La transformación de los materiales de partida en zeolitas ha sido evaluada por técnicas de difracción de rayos X de polvo, microscopia electrónica de barrido y espectroscopia de infrarrojo por transformada de Fourier para dilucidar el proceso de cristalización de zeolitas. El uso de materiales de bajo coste en la síntesis de zeolitas se ha convertido en un área de gran interés e investigación, desempeñando un papel activo en la promoción de los avances tecnológicos, la investigación y transferencia de tecnología relacionados con la producción de materiales zeolíticos en condiciones experimentales controladas.

Palabras clave: *Aluminosilicatos; Cristalización, Fusión, Hidrotermal, Zeolitas*

1. Introduction

Zeolites are abundant and widespread authigenic minerals formed from volcanic glass and various rock-forming minerals by interaction with aqueous solutions in a wide variety of geochemical environments, in particular, as alteration products of aluminosilicates (Mumpton, 1977). Natural zeolites have chemical and structural variations that must be related to the different geochemical environments in which they form (Kawano and Tomita, 1997). To clarify formation conditions of the variations of zeolites, numerous experimental studies on formation of zeolites have been conducted using starting materials such as natural and synthetic glasses, aluminosilicate gels, solution mixture and clay- and rock-forming minerals under a wide range of chemical and temperature conditions (Barrer, 1982).

The preparation of synthetic zeolites from silica and alumina chemical sources is expensive but has the advantage to produce materials of high-purity, with precisely engineered chemical and physical properties suitable for industrial applications and for scientific purposes. Therefore, in order to reduce costs, zeolite researchers are seeking cheaper raw materials for zeolite synthesis, which include clay minerals (Barrer, 1982; Breck, 1974; Boukadir *et al*., 2002; Klimkiewicz and Drąg, 2004; Ruiz *et al*., 1997; Baccouche *et al*., 1998; Cañizares *et al*., 2000), natural zeolites (Covarrubias *et al*., 2006), volcanic glasses (Aiello *et al*., 1982, 1984; Moirou *et al*., 2000), diatomite (Anderson *et al*., 2000, 2005), high silica bauxite (Puerto and Benito, 1996), oil shale (Shawabkeh *et al*., 2004) and natural clinker (Ríos, 2008; Ríos *et al*., 2008). The bulk chemical composition similarity of the starting materials with the volcanic materials from which the natural zeolites are originated by post-magmatic hydrothermal activity has motivated attempts to synthesize zeolytic materials, justifying the development of future investigations.

The increasing interest in zeolite synthesis from such low-cost materials has promoted the development of various studies on their conversion into zeolytic materials, giving rise to an extensive literature. Zeolite synthesis has been conventionally developed by hydrothermal reaction under alkaline conditions, as reported by several patents and scientific articles. However, the classic alkaline hydrothermal synthesis has been improved by using more sophisticated treatments, which include an alkaline fusion step followed by hydrothermal treatment, the application of microwave-assisted zeolite synthesis and the synthesis of zeolites under molten conditions without any addition of water (Shigemoto *et al*., 1993; Querol *et al*., 1997; Park *et al*., 2000a, 2000b).

Zeolites have been widely used as catalysts, adsorbents and ion-exchangers due to their unique porous structures and special acid–basic properties (Breck, 1974). Their use is becoming increasingly important in several environmental applications and thus is of increasing interest in water purification, particularly for the removal of ammonia, heavy metals, radioactive species and organic substances (Barrer, 1982; Breck, 1974).

Zeolites are crystalline aluminosilicates with open 3D framework structures built of SiO_4 and AlO_4 tetrahedra linked to each other by sharing all the oxygen atoms to form regular intracrystalline cages and channels of molecular dimensions. A defining feature of zeolites is that their frameworks are made up of 4-coordinated atoms forming tetrahedra. These tetrahedra are linked together by their corners and make a rich variety of beautiful structures, and they are the basic building blocks for various zeolite structures, such as the low-silica zeolites Na-A (LTA, Linde type A) and Na-X (FAU, faujasite), with a molar ratio of Si/Al of 1:1, which are the most common commercial adsorbents. As a consequence they contain the maximum number of cation exchange sites balancing the framework aluminum, and thus the highest cation contents and exchange capacities. Both Na-A and Na-X zeolite frameworks consist of corner sharing TO_4 tetrahedra (T = Si^{4+} or $Al3^{+}$).

The TO_4 tetrahedra are often referred to as the primary building units of these zeolite structures. Primary building units are linked together to form secondary building units.

The secondary building units consist of n-ring structures (4-ring for Na-A and 6-ring for Na-X), with each corner in the secondary building units representing the center of a tetrahedron. Secondary building units can be linked to form cages or channels within the structure. The aluminosilicate cages and the n-rings connect to form a three dimensional net type structure.

From the perspective of framework structure, both zeolites are stacked up by sodalite (SOD) cages (truncated octahedra) as shown in Figure 1, which can be described with the notation 4668 which means that it is composed of six 4-rings and eight 6-rings. The framework of zeolite Na-A contains two types of cages: β-cages (SOD) and α-cages (supercages of zeolite Na-A); β-cages are linked together by double four-membered rings (D4R) and form an inner cavity called supercage of zeolite Na-A, which has a diameter of 11.4 Å, is surrounded by 8 β-cages and is interconnected to six other supercages by 6-membered-ring windows. The framework of the zeolite Na-X consists of β-cages (SOD) and α-cages (supercages of zeolite Na-X); β-cages are linked together by double six-membered rings (D6R) and form the supercages of zeolite Na-X, which has a diameter of 13.0 Å, is surrounded by 10 β-cages and is interconnected to four other supercages by tetrahedrally disposed 12-membered-ring windows.

In this work, we investigate the hydrothermal transformation of kaolin and obsidian into zeolites Na-A and Na-X, respectively, following the alkaline fusion method. The crystallization mechanism of these zeotypes is also discussed.

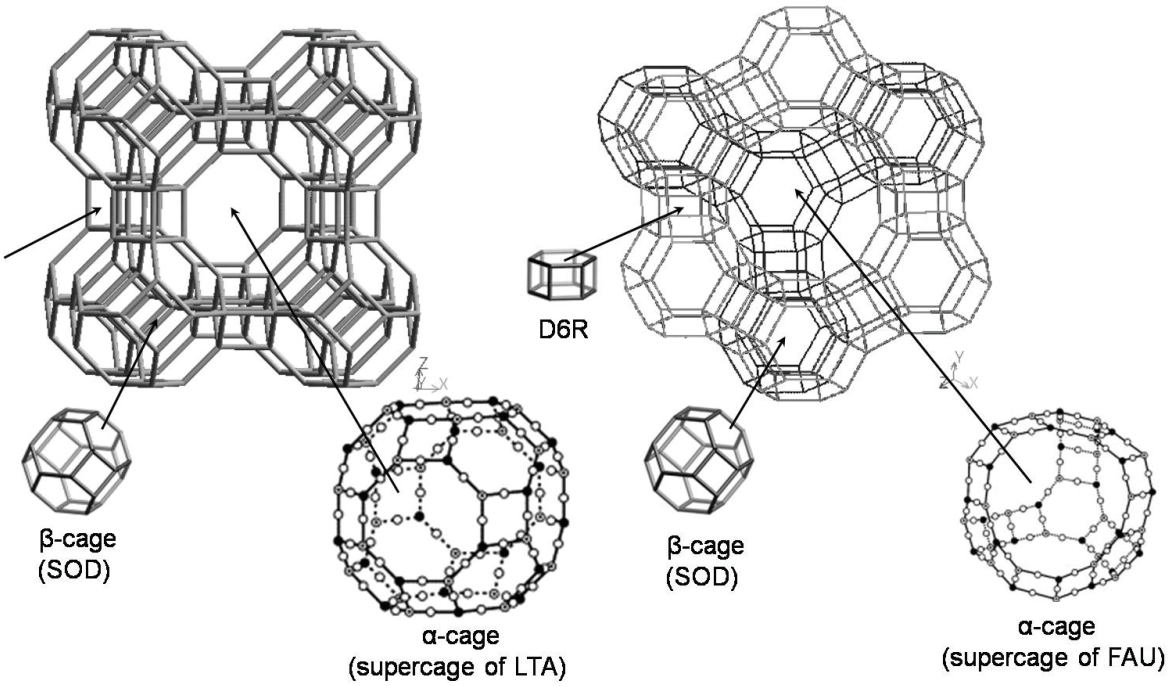

Figure 1. *Framework structures of zeolites Na-A (LTA) and Na-X (FAU), showing their characteristic cages and channels, adopted and modified from the Database of Zeolite Structures (http://www.iza-structure.org/databases/), Duan et al. (2007) and Nakano et al. (2010).*

2. Experimental

2.1 Materials and chemical reagents

Both kaolin and obsidian were used as starting materials in zeolite synthesis. Kaolin from South West England is distributed under the name of Supreme Powder and supplied by ECC International Ltd (chemical composition reported by Ríos *et al*., 2009a, 2009b: 46.44% SiO_2, 38.80% Al_2O_3, 0.03% TiO_2, 0.52% FeO, 0.08% MgO, 0.00% CaO, 0.33% Na_2O and 0.69% K_2O). Obsidian, a volcanic glass, from the Lipari Island (Eolie Archipelago, Italy) has

the following chemical composition: 75.27% SiO_2, 12.93% Al_2O_3, 0.08% TiO_2, 1.59% FeO, 0.00% MgO, 0.73% CaO, 4.13% Na_2O and 5.27% K_2O (Nielsen and Sigurdsson, 1981).

The aluminosilicate sources were prepared prior to the synthesis process as follows. Powder preparation techniques included both a SpectroMill Ball Pestle Impact grinder and a mortar and pestle. After grinding, samples were sieved under dry conditions and the size fraction of 200 mesh collected and particles of < 75 μm selected for zeolite synthesis. The dried powder samples were then ground as fine as possible, using a mortar and pestle, for further characterization. Sodium hydroxide (powder) 96% (BDH Laboratory Supplies) of analytical grade and distilled water were used in all experiments.

2.2 Synthesis of zeolites

We adopted in this study an alkaline fusion step prior to the hydrothermal treatment because it plays an important role in enhancing the hydrothermal conditions for zeolite synthesis and because larger amounts of aluminosilicates can be dissolved employing this method. In a typical synthesis process, 6.20 g of the raw material were dry mixed with 7.44 g of NaOH (powder) in a raw material/alkaline activator ratio = 1/1.2 in weight for 30 min and the resultant mixture was fused at 600 °C for 1 h. The alkaline reagent added to the starting material acts as an activator agent during fusion. Some of the inert crystalline phases in the raw materials can be fully reacted. The fused product was ground in a mortar and then 4.40 g of this was dissolved in 21.50 ml of distilled water (ratio = 1/4.9) under stirring conditions to form the amorphous precursors. The amount of reagents used for the preparation of the hydrogels was based on previous literature search (Shigemoto *et al*., 1993; Ríos, 2008; Ríos *et al*., 2009a, 2009b).

Hydrogels were aged under static conditions during 24 h. The hydrothermal reaction was carried out under static conditions, transferring the hydrogels to PTFE (polytetrafluoroethylene = Teflon) bottles (Cowie Technology Ltd) of 65 ml for preparations heated at the temperature required of 100 °C for different reaction times (24, 48, 96 h). The reactors were removed from the oven at the scheduled times and were quenched in cold water to stop the reaction. Hydrogel pH was measured before (14.1 for kaolin and 14.2 for obsidian) and after (13.8-14.0 for kaolin and 13.9-14.1 for obsidian) hydrothermal treatment. Then, the reaction mixtures were filtered and washed with distilled water to remove excess alkali. Finally, the samples were oven dried at 80 °C overnight. The dried samples were weighed and kept in plastic bags for characterization.

2.3 Characterization of the raw materials and as-synthesized zeolites

Powder X-ray diffraction patterns of the raw materials and as-synthesized products were recorded with a Philips PW1710 diffractometer operating in Bragg–Brentano geometry with Cu-Kα radiation (40 kV and 40 mA) and secondary monochromation. Data collection was carried out in the 2θ range 3–50°, with a step size of 0.02°. Phase identification was performed by searching the ICDD powder diffraction file database, with the help of JCPDS (Joint Committee on Powder Diffraction Standards) files for inorganic compounds. The morphological structure of the solid phases was examined by scanning electron microscopy (ZEISS EVO50) and the chemical composition of mineral phases was studied using the EDXS mode, under the following analytical conditions: I probe 1 nA, EHT=20.00 kV, beam current 100 μA, Signal A=SE1, WD=8.0 mm. Fourier transform infrared (FTIR) spectroscopy was carried out using a Mattson Genesis II FTIR spectrometer in the 4000-400 cm^{-1} region. However, we discuss only the 1200–400 cm^{-1} region where the spectra showed remarkable changes.

3. Results and discussion

3.1 Characterization of the starting materials

As shown in the XRD pattern (Figure 2a), kaolinite is the predominant mineral phase, which can be identified by its distinctive reflections at

12.34° and 24.64° of 2θ as reported by Zhao *et al*. (2004). However, minor impurities, such as illite, muscovite and halloysite, also occur. Kaolinite can be recognized by its platy morphology and hexagonal outlines (Figure 2a), with small well-formed hexagonal plates loosely packed, defining an orientation. XRD pattern of Figure 2b shows the entirely amorphous character of the obsidian, which is a non-hydrated silicate glass that have a three-dimensional disordered framework structure. SEM photograph (Figure 2b) of this glass show nearly planar surfaces that have irregularities.

3.2 Characterization of the zeolytic materials

The XRD patterns in Figure 3 show the progress of zeolite synthesis by the fusion method, revealing the reduction of intensity of the characteristic peaks of the starting materials and the appearance of new reflection peaks corresponding to zeolites Na-A and Na-X, which show a progressive increase in the intensity with reaction time. Therefore, the reaction time influences the crystallinity of the synthesis products. Figure 3a reveals a total dissolution of the kaolin-bearing phases. Note

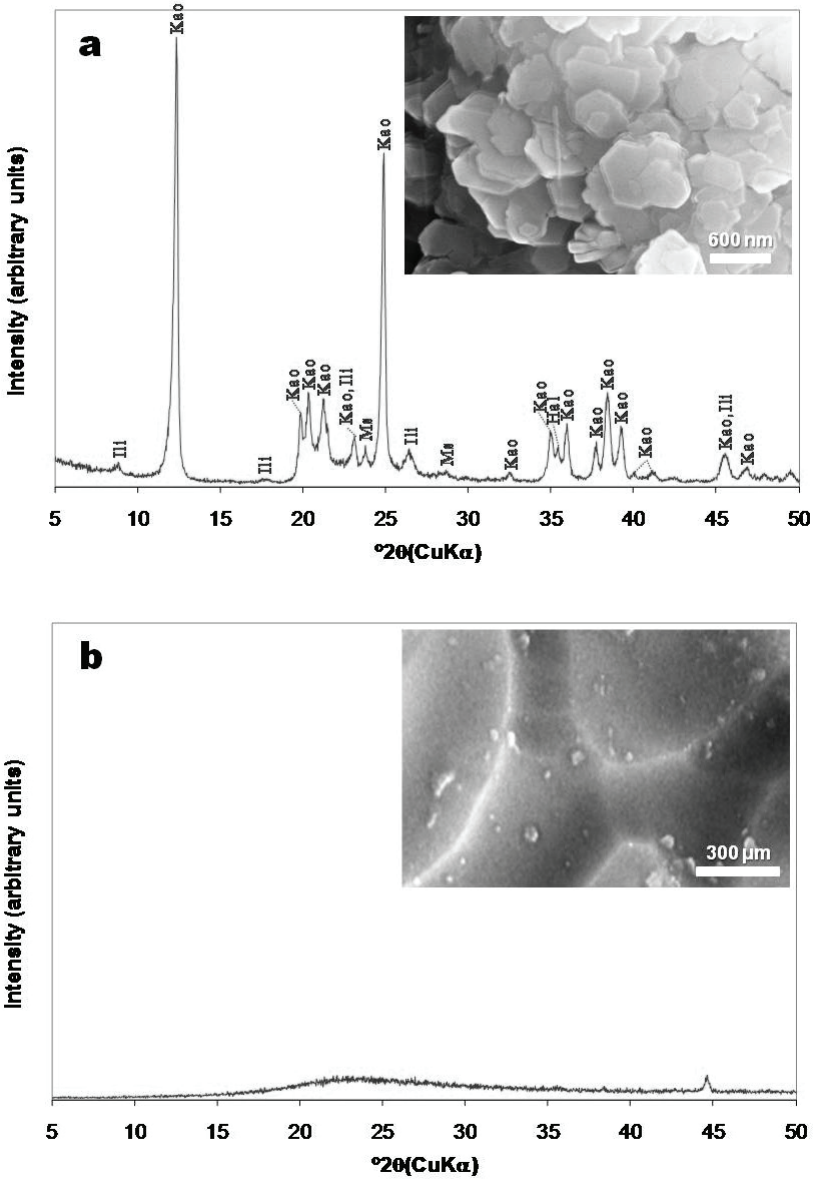

Figure 2. *X-ray diffraction patterns and SEM images of the starting materials: (a) kaolin and (b) obsidian. Kao, kaolin; Ill, illite; Ms, muscovite; Hal, halloysite.*

the intensities of strong characteristic diffraction peaks for zeolite Na-A, which appeared after 24 h, keeping a constant grade of crystallinity with reaction time. On other hand, Figure 3b shows that after 24 h of reaction a displacement of the hump of the starting material to higher 2-theta values was observed. However, with reaction time a progressive transformation from an amorphous phase to a crystalline phase (zeolite Na-X) occurred after 48 h. The intensities of the reflections peaks of zeolite Na-X increase from 48 to 96 h.

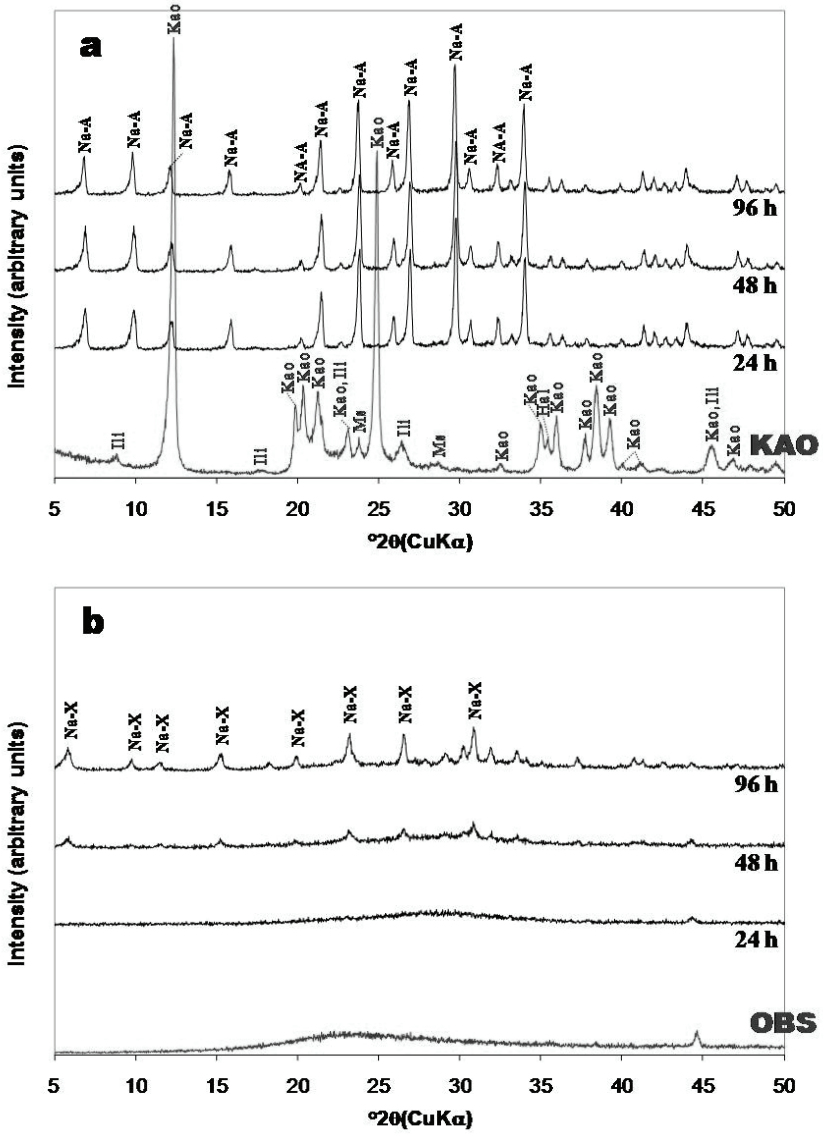

Figure 3. *X-ray diffraction patterns of Na-A and Na-X zeolites synthesized from (a) kaolin and (b) obsidian, respectively.*

The synthesis of zeolites via alkaline fusion followed by hydrothermal treatment reveals that the alkaline fusion process promoted the dry reaction between the mineral phases present in the raw materials and the alkaline activator, and the alkaline fused product corresponds to amorphous sodium aluminosilicate (SEM images), indicating that fusion was very effective in extracting the silicon and aluminium species from kaolin. SEM images of the morphology of the as-synthesized zeolytic products obtained after activation of the starting materials are exhibited in Figure 4. Figure 4(a-b) shows the typical morphology of well-developed cubes of zeolite Na-A displaying fluorite-type interpenetration-twinning, similar to those reported in previous studies (Gerson and Zheng, 1997; Porcher *et al*., 2000; Zhao *et al*., 2004).

Twinned crystals of zeolite Na-A are of the same size and correspond to an intergrowth of two cubes like that found in twinned fluorite crystals. Using obsidian as starting material, the authors have observed that poor crystalline zeolite Na-X is the single phase in the synthesis products. However, this zeolite type does not show its characteristic octahedral morphology, as shown in Figure 4(c-d).

The presence of aluminosilicate framework in the zeolites was confirmed using the FTIR spectroscopic technique and the results are shown in Figure 5. The internal tetrahedral bending peak (~ 464 cm^{-1}) for kaolin does not exists in the synthesis products shifts from 456 to 459 cm^{-1} due to the incorporation of alumina tetrahedron into the zeolite framework. The vibration band at 433 cm^{-1} for obsidian changed to 411 (amorphous material) and 439-449 (zeolite Na-X) cm^{-1}. The emergence of crystal phase is characterized by the double ring external linkage peak (543-545, 552 and 599 cm^{-1}), internal linkage symmetrical stretching peak (652-658 and 660-677 cm^{-1}), external tetrahedral symmetrical stretching peak (733 cm^{-1}) and internal tetrahedral asymmetrical stretching peak (966-981 and 973-986 cm^{-1}). Observe how the peaks change suddenly from 24 to 48 h using obsidian, taking into account that after 24 h the synthesis product corresponds to an amorphous material, whereas after 48 h zeolite Na-X appears. During hydrothermal reaction, the characteristic vibration bands of the raw materials disappeared, accompanied by zeolite crystal grow rapidly. It means that the formation of the zeolite crystal happens very quickly in the synthesis solution. The six-membered rings, as secondary building unit of the zeolite, are formed during the induction period, while the double ring structure, tertiary building unit of these zeolites, is formed afterwards (Hu *et al*., 2009). All these observations confirm the formation of zeolites Na-A and Na-X after alkali fusion followed by hydrothermal treatments of the raw materials. The different intensity of the vibration bands of the synthesis products confirms XRD patterns concern with the grade of crystallinity.

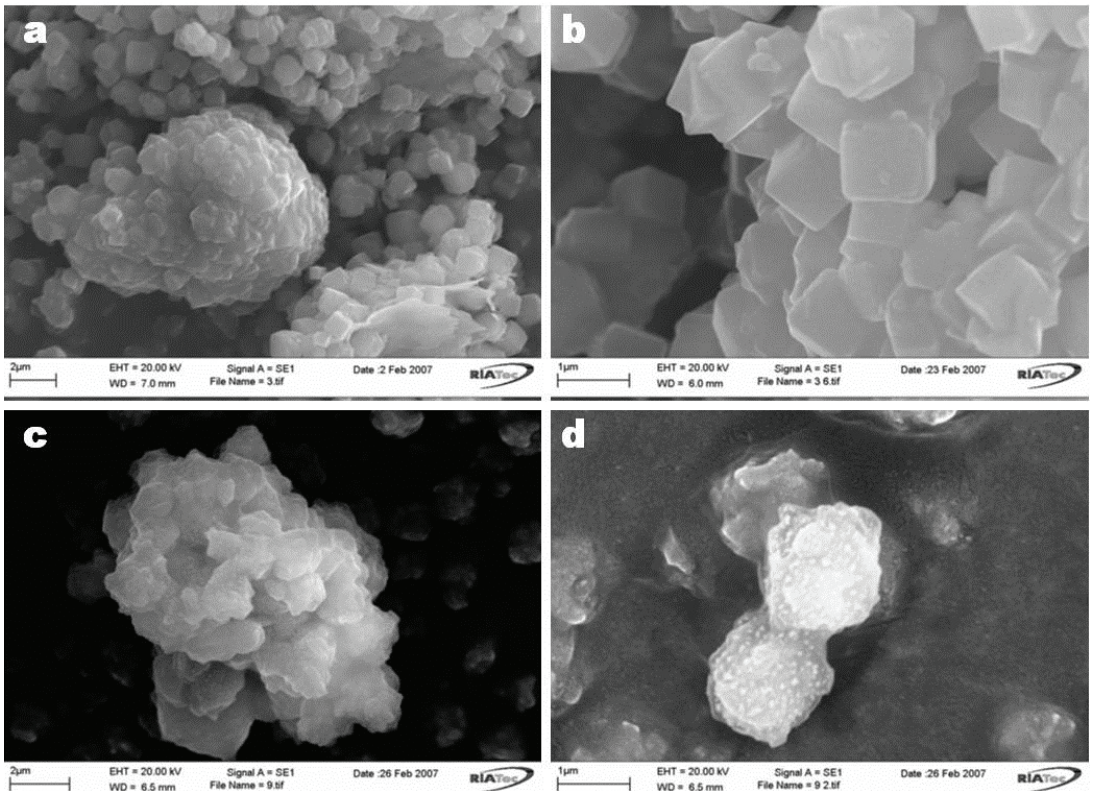

Figure 4. *SEM images of the as-synthesized zeolites Na-A (a-b) obtained from kaolin at 60oC after 96h and Na-X (c-d) obtained from obsidian at 60oC after 96h.*

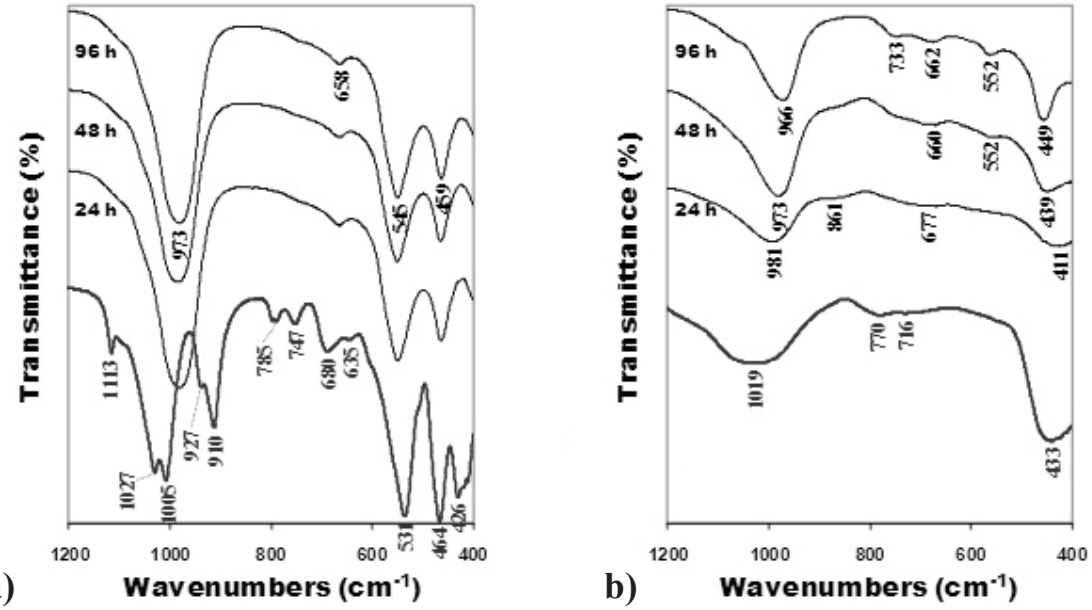

Figure 5. *FTIR spectra of the unreacted raw materials (in red) and representative as-synthesized products obtained from (a) kaolin and (b) obsidian.*

3.3 Reaction mechanism during zeolite synthesis

The reaction mechanism of zeolite synthesis from kaolin and obsidian via alkaline fusion prior to hydrothermal reaction is discussed here and can be divided into a number of steps: fusion of the starting material with NaOH, dissolution of the alkaline fused product releasing Si and Al (preparation of the reaction gel) and hydrothermal reaction at 80 ºC for several reaction times (24, 48 and 96 h).

The chemistry of evolution of the system, such as zeolites Na-A and Na-X, is very complex due to several factors, such as impurities present in the starting materials, gel composition and pH, aging conditions, reaction temperature and time, formation of intermediate metastable phases, and nucleation and growth of more stable phases, among others. However, the reaction history of the zeolite synthesis can be summarized as follows. A simple scheme of the crystallization of an amorphous aluminosilicate hydrogel to zeolites Na-A and Na-X is given in Figure 6.

The alkaline fusion (solid-state reaction) step at 600 °C (Figure 6a) enhances the dissolution of the Al_2O_3 and SiO_2 from the starting materials, mostly converting them into sodium salts (Na_2SiO_3 + Na_2AlO_2)

The step of gel preparation (Figure 6b), Na_2SiO_3 + Na_2AlO_2 are dissolved in H_2O at room temperature to produce the reaction gel with a chemical composition, which can be expressed as $[Na_x(AlO_2)_y(SiO_2)_z.NaOH.H_2O]_{(gel)}$ as suggested by Kondru *et al*. (2011).

During the formation of zeolites Na-A and Na-X in the hydrothermal reaction, the following events occur: induction period, which is followed by nucleation and crystal growth. For the induction period, reaction intermediates remain mostly amorphous as a gel, prior to crystallization. According to Epping and Chmelka (2006), with the onset of crystallization, most of the intermediate gel transforms relatively rapidly to crystalline zeolytic product. This process appears to occur more rapidly in more concentrated gels, in which a greater number of small crystalline nuclei are expected to form during the induction period (Shi *et al*., 1996). During the induction period, a reorganization of the amorphous aluminosilicate gel occurred. It can lead to the formation of "crystalline" zeolite nanoparticles throughout the amorphous gel (Epping and Chmelka, 2006).

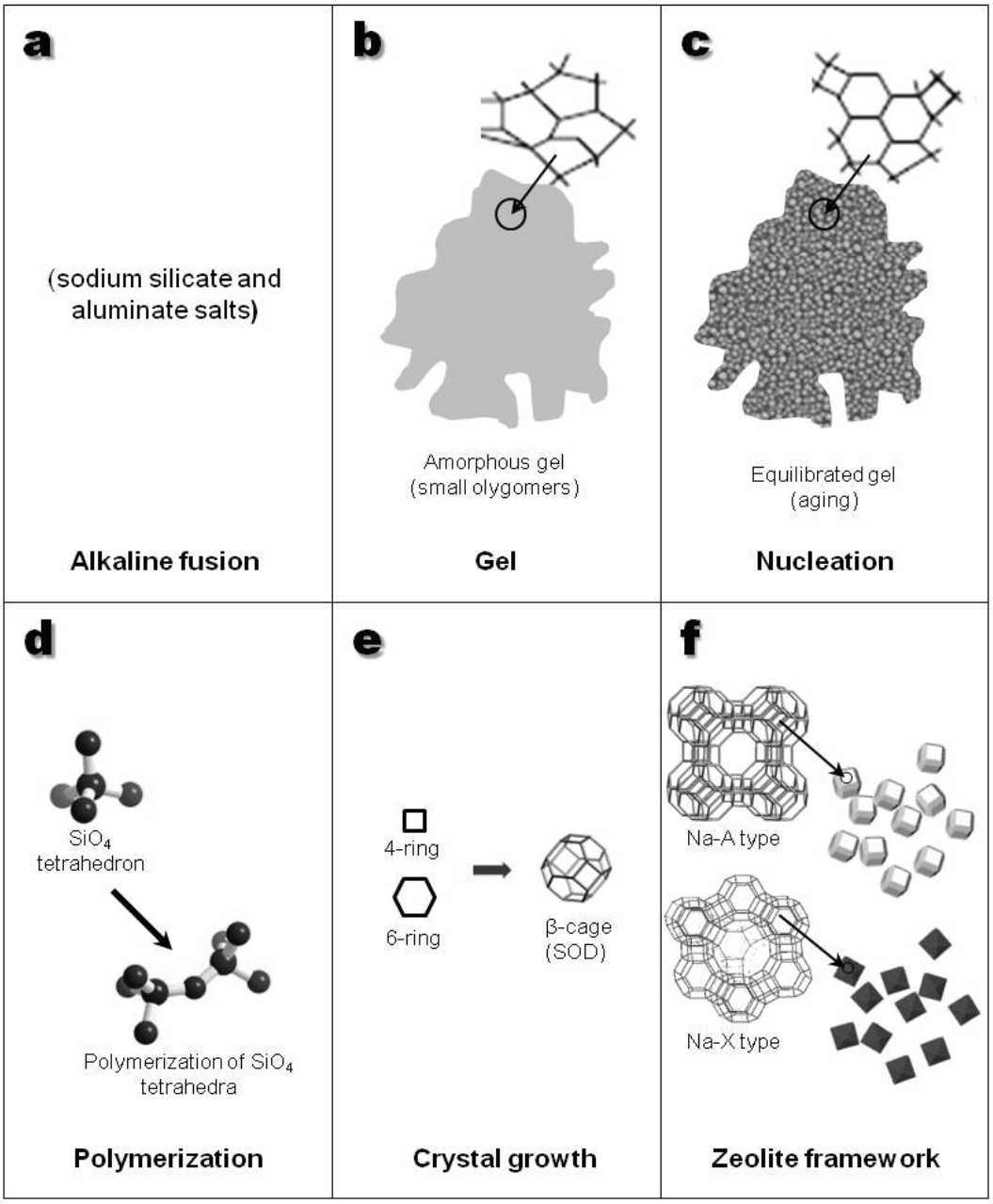

Figure 6. *Schematic picture of the crystallization mechanism of zeolites Na-A and Na-X.*

Nucleation is a phase transition where a semiordered gel is transformed in a structure sufficiently ordered to germ nuclei (Figure 6c), which become larger with time. The crystallization of zeotype materials is frequently constrained by limitations at the nucleation stage so that it is common practice to age reaction mixtures (Barrer, 1982). There are two potential effects of this procedure on the synthesis reaction: (a) reduction of the induction period preceding the detection of crystalline product and (b) promotion of a dominant crystalline phase; thus, overall synthesis time can be shortened and product purity improved (Cundy *et al*., 1998).

A polymerization (Figure 6d) should be the process that forms the zeolytic precursors, which contains tetrahedra of Si and Al randomly distributed along the polymeric chains that are cross-linked so as to provide cavities sufficiently large to accommodate the charge balancing alkali ions. It is well known that zeolites are based on the primary tetrahedral building unit

(TO_4) where the central tetrahedrally bonded (T) atom is usually either a silicon or aluminium atom, surrounded by four oxygen atoms. By linking these tetrahedra together, it is possible to build larger structures, as shown in Figure 6d. According to Itani *et al*. (2009), during the initial polymerization of aluminosilicate species a significant part of the Na^+ is expelled from the gel into the solution, which restricts extensive polymerization and leads to formation of small aluminosilicate particles with open pore structure.

During nucleation, the gel composition was significantly affected by thermodynamic and kinetic parameters (Ojha *et al*., 2004). Gel composition and structure are significantly affected by thermodynamic and kinetic parameters. According to Breck (1974), they are controlled by the size and structure of the polymerization species and gelation controls the nucleation of the zeolite crystallites. When the TO_4 units are linked together to form a zeolite framework, they characteristically yield periodic cavities and channels throughout the structure (Figure 6e).

The primary TO_4 units can be linked to create secondary building units (SBU's). In zeolites Na-A and Na-X, a combination of 4- and 6-rings promoted the formation of the β-cage. Crystallization generally involved the assimilation of material from solution by a crystal growth process, which began when the nuclei reached a critical size and the crystals started to grow. A stable phase reached the required equilibrium conditions to promote the crystal growth of zeolites Na-A and Na-X. The lineal growth rates of zeolites show a strong dependence with temperature. However, these rates are also influenced by several variables, particularly the molar composition of the reaction gel. The hydrothermal treatment of the reaction gel at the scheduled temperature and time of reaction produced the crystallization of zeolites Na-A and Na-X. The Na^+ cation also plays a very important role during zeolitization, because it stabilizes the sub-building units of zeolite frameworks and is fundamental for zeolite synthesis under hydrothermal conditions (Fernández-Jiménez *et al*., 2005). We are in agreement with Smaihi *et al*. (2003) that the first crystallization stage proceeds by reorganization of the amorphous aluminosilicate units formed during the mixing of the precursors. The crystallization process takes place in the volume of the aggregates by propagation through the gel phase (Smaihi *et al*., 2003). This propagation through the gel continues to complete the transformation of the particles into zeolites Na-A and Na-X. After this stage, the growth in the system is dominated by the solution-mediated transport, which leads to the crystallization of well-shaped crystals of zeolites Na-A and Na-X and consequently their structures (Figure 6f).

4. Potential environmental applications of the synthesized zeolytic materials

Major prospective applications of the synthesized zeolytic materials are based on their use as high ion exchangers in industrial wastewater and soil decontamination. Previos studies by Ríos and co-workers (Ríos, 2008; Ríos *et al*., 2008; Contreras and Castrillon, 2011) reveal that the use of zeolites Na-A and Na-X may be an alternative to heavy metal removal from industrial wastewater. In general, the results are very encouraging about the future industrial applications of the synthesized zeolytic materials. The further investigation of the synthesized zeolytic materials, which will be conducted in the near future, includes the test of their ability of precipitating or adsorbing heavy metals from industrial wastewaters.

5. Conclusions

Both kaolin and obsidian are suitable as raw materials for the synthesis of pure zeolites Na-A and Na-X in the system of SiO_2-Al_2O_3-Na_2O-H_2O using NaOH as activating agent and an alkaline fusion step followed by hydrothermal treatment. By fusion with NaOH powder, mineral phases in the starting materials can be completely changed into a Na aluminosilicate. The synthesis method introducing an alkaline fusion step prior to the hydrothermal treatment produced crystalline zeolites after short times of crystallization. The results obtained in this study prove that further studies should be

carried out under well-optimized experimental conditions to successfully prepare highly crystalline zeolites with potential application in the purification of industrial wastewater.

6. Acknowledgments

This research was supported by the Programme Alban, "the European Union Programme of High Level Scholarships for Latin America" (Scholarship No. E05D060429CO) and the Universidad Industrial de Santander, and has benefited from research facilities provided by the School of Applied Sciences at the University of Wolverhampton. The authors are indebted to Dr. David Townrow, Mrs Diane Spencer, and Mrs. Barbara Hodson for their technical assistance with the acquisition of XRD, FTIR and SEM data. We are most grateful to the above-named people and institutions for support.

7. References

Aiello, R., Nastro, A., Crea F., & Colella, C. (1982). Use of natural products for zeolite synthesis. V. Self-bonded zeolite pellets from rhyolitic pumice. *Zeolites* 2 (4), 290-294.

Aiello, R., Nastro, A., Crea F., & Colella, C. (1984). Use of natural products for zeolite synthesis. VI. Zeolite microcrystals from rhyolitic pumice grains. *Materials Letters* 2 (6), 529-533.

Anderson, M.W., Holmes, S.M., Hanif, N., & Cundy, C.S. (2000). Hierarchical Pore Structures through Diatom Zeolitization. *Angewandte Chemie* 39 (15), 2707-2710.

Anderson, M.W., Holmes, S.M., Mann, R., Foran, P., & Cundy, C.S. (2005). Zeolitisation of diatoms. *Journal of Nanoscience and Nanotechnology* 5 (1), 92-95.

Baccouche, A., Srasra E., & Maaoui, M.E. (1998). Preparation of Na-P1 and sodalite octahydrate zeolites from interstratified illite–smectite. *Applied Clay Science* 13 (4), 255-273.

Barrer, R.M. (1982). Hydrothermal Chemistry of Zeolites, First edition, New York: Academic Press.

Boukadir, D. Bettahar, N., & Derriche, Z. (2002). Synthesis of zeolites 4A and HS from natural materials. *Annales de Chimie Science des Materiaux* 27 (4), 1-13.

Breck, D.W. (1974). Zeolite Molecular Sieves: Structure, Chemistry and Use. First edition, New York: John Wiley.

Cañizares, P., Durán, A., Dorado, F., & Carmona, M. (2000). The role of sodium montmorillonite on bounded zeolite-type catalysts. *Applied Clay Science* 16 (5-6), 273–287.

Contreras, V.D., & Castrillon, Y.P. (2011). Síntesis de zeolita tipo fauajasita a partir de la activación alcalina de illita para su aplicación en la eliminación de Cr^{3+} y Ni^{2+} de efluentes de la industria del galvanizado. Tesis de pregrado, Universidad Industrial de Santander, Bucaramanga, Colombia.

Covarrubias, C., Garcia, R., Arriagada, R., Yanez, J., & Garland T. (2006). Cr(III) exchange on zeolites obtained from kaolin and natural mordenite. *Microporous and Mesoporous Materials* 88 (1-3), 220-231.

Cundy, C.S., Plaisted, R.J., & Zhao, J.P. (1998). Remarkable synergy between microwave heating and the addition of seed crystals in zeolite synthesis - a suggestion verified. *Chemical Communications* (14), 1465-1466.

Database of Zeolite Structures. http://www.iza-structure.org/databases/ 18 June 2011.

Duan, T.C., Nakano, T., & Nozue, Y. (2007). Evidence for ferromagnetism in rubidium clusters incorporated into zeolite A. *Journal of Magnetism and Magnetic Materials* 310 (2), 1013–1015.

Epping, J.D., & Chmelka, B.F. (2006). Nucleation and growth of zeolites and inorganic mesoporous solids: Molecular insights from magnetic resonance spectroscopy. *Current Opinion in Colloid & Interface Science* 11 (2-3), 81–117.

Fernández-Jiménez, A., Palomo, A., & Criado, M. (2005). Microstructure development of alkali-activated fly ash cement: a descriptive model. *Cement and Concrete Research* 35 (6), 1204-1209.

Gerson, A.R., & Zheng K. (1997). Bayer process plant scale: transformation of sodalite to cancrinite. *Journal of Crystal Growth* 171 (1-2), 209–218.

Hu, L., Xie, S., Wang, Q., Liu, S., & Xu, L. (2009). Phase selection controlled by sodium ions in the synthesis of FAU/LTA composite zeolite. *Science and Technology of Advanced Materials* 10, 1-8.

Itani, L., Liu, Y., Zhang, W., Bozhilov, K.N., Delmotte, L., & Valtchev, V. (2009). Investigation of the physicochemical changes preceding zeolite nucleation in a sodium-rich aluminosilicate gel. *Journal of the American Chemical Society* 131 (29), 10127-10139.

Kawano, M., & Tomita K. (1997). Experimental study on the formation of zeolites from obsidian by interaction with NaOH and KOH solutions at 150 and 200 ^{o}C. *Clays and Clay Minerals* 45 (3), 365-377.

Klimkiewicz, R., & Drąg, E.B. (2004). Catalytic activity of carbonaceous deposits in zeolite from halloysite in alcohol conversions. *Journal of Physics and Chemistry of Solids* 65 (2-3), 459-464.

Kondru, A.K., Kumar, P., Teng, T.T., Chand, S., & Wasewar, K.L. (2011). Synthesis and characterization of Na-Y zeolite from coal fly ash and its effectiveness in removal of dye from aqueous solution by wet peroxide oxidation. *Archives of Environmental Science* 5, 46-54.

Moirou, A., Vaxevanidou, A., Christidis, G.E., & Paspaliaris, I. (2000). Ion exchange of zeolite Na-Pc with Pb^{2+}, Zn^{2+} and Ni^{2+} ions. *Clays and Clay Minerals* 48 (5), 563-571.

Mumpton, F.A. (1977). Mineralogy and geology of natural zeolite. *Reviewes in Mineralogy. Short Course Notes* 4. Virginia: Mineralogical Society of America.

Nakano, T., Mizukane, T., & Nozue, Y. (2010). Insulating state of Na clusters and their metallic transition in low-silica X zeolite. *Journal of Physics and Chemistry of Solids* 71 (4), 650–653.

Nielsen, C.H., & Sigurdsson, H. (1981). Quantitative methods for electron microprobe analysis of sodium in natural and synthetic glasses. *American Mineralogist* 66, 547-552.

Ojha, K., Pradhan, N.C., & Samanta, A.N. (2004). Zeolite from fly ash: synthesis and characterization. *Bulletin of Material Science* 27 (6), 555–564.

Park, M., Choi, C.L., Lim, W.T., Kim, M.C., Choi, J., & Heo, N.H. (2000a). Molten-salt method for the synthesis of zeolitic materials: I. Zeolite formation in alkaline molten-salt system. *Microporous and Mesoporous Materials* 37 (1-2), 81-89.

Park, M., Choi, C.L., Lim, W.T., Kim, M.C., Choi, J., & Heo, N.H. (2000b). Molten-salt method for the synthesis of zeolitic materials: II. Characterization of zeolitic materials. *Microporous and Mesoporous Materials* 37 (1-2), 91-98.

Porcher, F., Dusausoy, Y., Souhassou, M., & Lecomte C. (2000). Epitaxial growth of zeolite X on zeolite A and twinning in zeolite A: structural and topological analysis. *Mineralogical Magazine* 64 (1), 1-8.

Puerto, R.A., & Benito, J.F. (1996). Manufacture of zeolite 4A from bauxite. *Zeolites* 17 (3), 315-315.

Querol, X., Plana, F., Alastuey, A., Lopez-Soler, A., Plana, F., Andres, J.M., Juan, R., Ferrer, P., & Ruiz, C.R. (1997). A fast method of recycling fly ash: microwave assisted zeolite synthesis. *Environmental Science & Technology* 31 (9), 2527-2532.

Ríos, C.A. (2008). Synthesis of zeolites from geological materials and industrial wastes for potential application in environmental problems. PhD Thesis, University of Wolverhampton, Wolverhampton, England.

Ríos, C.A., Williams, C.D., & Roberts, C.L. (2008). Removal of heavy metals from acid mine drainage (AMD) using coal fly ash, natural clinker and synthetic zeolites. *Journal of Hazardous Materials* 156 (1-3), 23–35.

Ríos, C.A., Williams, C.D., & Fullen, M.A. (2009a). Nucleation and growth history of zeolite LTA synthesized from kaolinite by two different methods. *Applied Clay Science* 42 (3-4) 446-454.

Ríos, C.A., Williams, C.D., & Fullen, M.A. (2009b). Hydrothermal synthesis of hydrogarnet and tobermorite at 175 °C from kaolinite and metakaolinite in the CaO-Al_2O_3-SiO_2-H_2O system: A comparative study. *Applied Clay Science* 43 (2), 228-237.

Ruiz, R., Blanco, C., Pesquera, C., Gonzalez, F., Benito, I., & Lopez, J.L. (1997). Zeolitization of a bentonite and its application to the removal of ammonium ion from waste water. *Applied Clay Science* 12 (1), 73-83.

Shawabkeh, R., Al-Harahsheh, A., Hami, M., & Khlaifat, A. (2004). Conversion of oil shale ash into zeolite for cadmium and lead removal from wastewater. *Fuel* 83 (7-8), 981-985.

Shi, J. Anderson, M.W., & Carr, S.W. (1996). Direct observation of zeolite A synthesis by in situ solid-state NMR. *Chemistry of Materials* 8 (2), 369-375.

Shigemoto, N., Hayashi, H., & Miyaura, K. (1993). Selective formation of Na-X zeolite from fly ash by fusion with sodium hydroxide prior to hydrothermal reaction. *Journal of Materials Science* 28, 4781-4786.

Smaihi, M., Barida, O., & Valtchev, V. (2003). Investigation of the Crystallization Stages of LTA-Type Zeolite by Complementary Characterization Techniques. *European Journal of Inorganic Chemistry* 24, 4370-4377.

Zhao, H., Deng, Y., Harsh, J.B., Flury, M., & Boyle, J.S. (2004). Alteration of kaolinite to cancrinite and sodalite by simulated Hanford tank waste and its impact on cesium retention. *Clays and Clay Minerals* 52 (1), 1–13.